Improving Ducting to Increase Cooling Performance of High-End Web Servers Subjected to Significant Thermal Shadowing - An Experimental and Computational Study

by

DIVYA MANI

Presented to the Faculty of the Graduate School of
The University of Texas at Arlington in Partial Fulfillment
of the Requirements
for the Degree of

MASTER OF SCIENCE IN MECHANICAL ENGINEERING

THE UNIVERSITY OF TEXAS AT ARLINGTON

December 2014

Dedicated to The Almighty and my loving parents Mr. Mani and Ms. Selvi

ACKNOWLEDGEMENTS

I would like to thank Dr. Dereje Agonafer for his continuous guidance, support and encouragement over the last two years of my research work in University of Texas at Arlington. I would also like to thank him for providing me a lot of opportunities to attend conferences and workshops.

I would like to thank Dr. Haji-Sheikh and Dr. Kent Lawrence for serving my thesis committee. I would also like to take the opportunity to thank Dr.Veerendra mulay for providing me opportunity to work on Facebook servers and for continuous guidance and feedback. I am thankful to Ms. Sally Thompson for helping me in various educational matters.

I am obliged and thankful to John Fernandes for sharing his technical expertise throughout my research work. His mentoring and support has played a important role in finishing this work.I would also like to than Richard Eiland for sharing his ideas and technical expertise.

My special thanks to my parents Mr. S. M. Mani and M. Selvi, my sister Deepika and my brother Dinesh for serving my motivation and inspiration. I endlessly thank them for providing an opportunity to pursue my goals in life. This acknowledgment would not be complete without expressing my gratitude to the Almighty, who has been constantly showing me right path in my life and for providing me strength and courage to face any situations in life to reach my goals.

October 23, 2014

ABSTRACT

Improving Ducting to Increase Cooling Performance of High-End
Web Servers Subjected to Significant Thermal Shadowing
- An Experimental and Computational Study

Divya Mani, M.S.
The University of Texas at Arlington, 2014

Supervising Professor: Dereje Agonafer

Ensuring that all the critical components like CPU's receive sufficient amount of flow as per their requirement is an vital importance in implementing air cooling for IT equipments.In addition to that the overall system resistance varies with the component location within the chassis. In this study, parametric improvement in chassis ducting system is made to counteract the effects of thermal shadowing in a open compute air cooled server in which a CPU thermally shadows the other.

Commercially available computational fluid dynamics codes have permitted simulation of server models to predict efficiency of the servers with every changes made in the design and input variables. Initially this study discusses about the methodology that outlines experimental procedures and tests employed for generating data for calibration of a detailed server model generated using a commercially available CFD tool. The resulting experimentally-calibrated computational fluid dynamics model of the server is used to parametrize and improve the duct design and the location with the view of estimating the effect of airflow bypass on fan power

consumption and CPU die temperatures. Improvements achieved are experimentally tested by prototyping the improved chassis using acrylic sheets and reported with reduced flow rates, flow speeds, fan power consumption and fan acoustic noise levels.

Further, the study is extrapolated for evaluating the savings in total pumping power and flow rates in the layout of a traditional data center and highly-efficient data center working on air side economization. Savings in amount of water consumed by the layout and savings in number of computer room air conditioning(CRAC) units are also evaluated.

TABLE OF CONTENTS

LIST OF ILLUSTRATIONS

LIST OF TABLES

CHAPTER 1

Introduction

1.1 Data Center: An Introduction

Datacenter is a huge facility which houses a large number of rack mount servers to store, manage and process data. Computer dependent demands in the past few years has encouraged the rapid growth of datacenters in almost all the sectors like financial services, media, universities and government Infrastructures. Adding to this, the growing environmental concerns and increase in energy cost and power consumptions simultaneously has triggered the datacenter professionals to strive hard to develop more efficient power and cooling technologies .

Recent survey by Kooney reported that in 2010, the electricity utilized by datacenters accounted for between 1.1% -1.5% and 1.7% -2.2% of the total energy consumption in the World and in United States respectively [1]. A survey conducted by Digital Reality Trust, on 300 North American corporations reported a PUE of 2.9, which means 1.9 extra watts were consumed by the firms for every watt used to power the servers [2]

All the IT equipments employed in datacenters consume tremendous power and dissipate enormous amount of heat which needs to be cooled continuously to maintain the reliability of the components. To ensure effective cooling performance, it is necessary to supply sufficient air flow to these components as per their requirements. Therefore airflow management is very important criteria to be considered at all the levels of the datacenter. Another important parameter which decides the efficiency and performance of the server is the temperature of ambient air entering the IT

equipment. ASHRAE TC 9.9 has classified four classes which define allowed and recommended temperature ranges for datacenter applications. Inlet temperatures can be selected from any of the four zones (A1, A2, A3 and A4) as shown in Figure 1.1 depending on the operators applications [3].

An energy Logic model by Emerson Network Power, reported that one Watt of power saved at the server level extrapolated to as much as 2.84 watts at the facility level [4] Every year new guidelines are designed by the datacenter industry officials to maximize the performance of the datacenters. But still, increasing the efficiency of the IT equipment at the server level would scale the performance to a larger extent at the facility level of a datacenter.

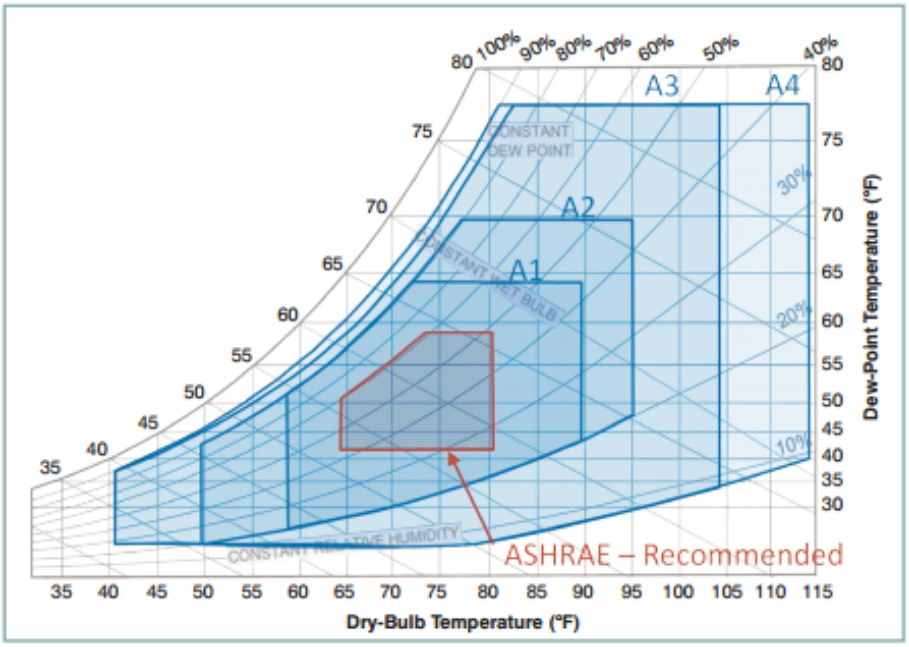

Figure 1.1. 2011 ASHRAE environmental classes for data center applications).

1.2 Air Cooling Configuration

In an air cooled server, the cooling system comprises of heat sinks and axial fans. Basically Heat sinks aid the heat transfer from the processors to ambient through conduction, convection and radiation process and fans are used to drive air through the server components carrying heat generated by components from inlet to outlet of the server. Usually in an air cooled server, the major contributor of system resistance is the heat sinks. The fans are usually controlled by the processor temperatures with the help of inbuilt fan control algorithms. Further, the exhaust hot air from the server enters the hot aisle in a datacenter room and is sent to the Computer Room Air conditioning (CRAC) units to cool the air to required inlet temperatures. The cooled air from the CRAC Units is then delivered to cold aisles through perforated tiles. A typical design datacenter room is shown in Figure 1.2 [5] .

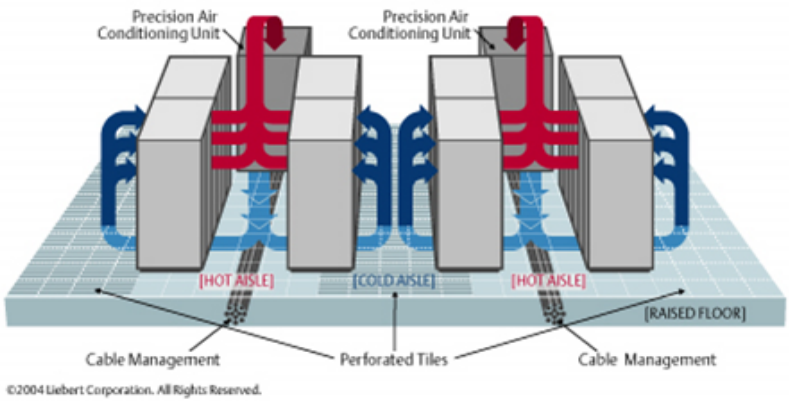

Figure 1.2. Hot aisle/ Cold aisle approach.

1.3 Effects of Flow Bypass and Thermal Shadowing

The heat transfer rate of the heat sinks varies proportionally to the velocity of air flowing across the heat sink fins. The bypass area around the heat sink is usually quantified as tip clearance and span wise spacing which governs the flow bypass around the heat sink. Excessive flow bypass leads to reduced velocity of air through the fins which in turn results in poor heat transfer from the processors to the ambient. Therefore to achieve higher cooling performance through the heat sinks, flow bypass should be carefully studied and should be maintained as minimal as possible.

$h = f\ (V_{ch})$

On the other hand, in a parallel heat sink configuration, the upstream heat sink (region 0) thermally shadows the downstream heat sink (Region 1) as seen in Figure 1.3. The heat dissipated by the CPU in Region 0, is carried away by air passing through upstream heat sink, through convection process. The hot air from this heat sink mixes with the cold bypass air and the resulting warm air enters the downstream heat sink. Therefore due to higher heat sink inlet temperature, the temperature difference across downstream heat sink reduces and results in a reduced heat transfer effect. Usually the server fans are controlled by the processor temperatures. As the processor temperatures increase, the fan speeds ramp up to keep the processors within their specified temperatures. Therefore, poor cooling performance on components leads to increase in fan power consumption, due to the fact that fan speeds varies non linearly to its power consumption. To summarize this, excessive increase in bypass of the cold air in region 1 would result in velocity loss in upstream heat sink, but at the same time , excessive reduction in cold air mixing with the hot air coming from upstream heat sink would result in higher inlet temperature of air entering downstream heat sink. Therefore to reduce processor temperatures and to achieve

better cooling performance, the air flow mixtures should be analyzed effectively and carefully.

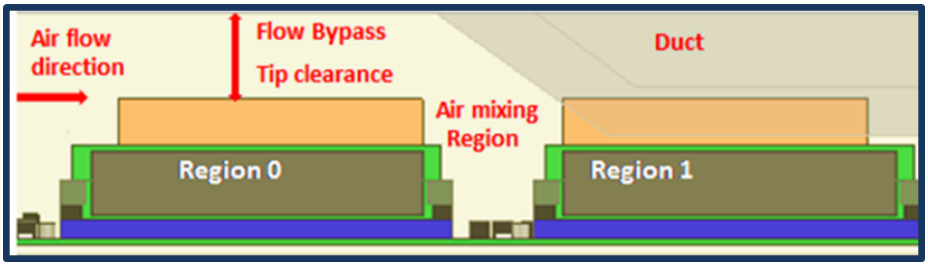

Figure 1.3. Side view representing flow bypass and air mixing zones.

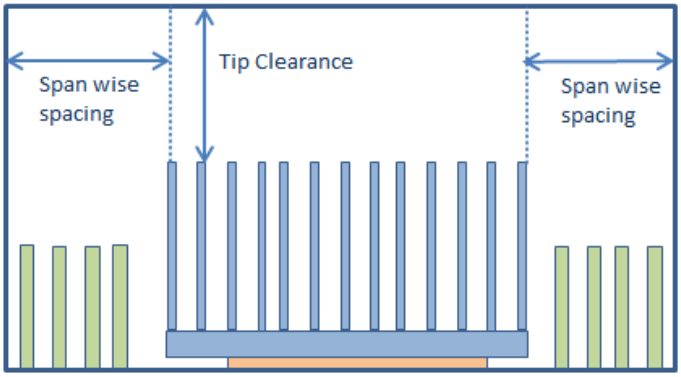

Figure 1.4. Front View of heat sinks and DIMMS showing tip clearance and span wise spacing.

1.4 Motivation of the work

A datacenter infrastructure houses thousands and thousands of servers. And therefore small savings achieved at the server level would save enormous capital investment at the data center infrastructure level.The Sever fans are controlled by the processor temperatures using inbuilt fan control algorithms. Higher processor tem-

peratures require the fan to spin at a higher speed which means higher fan power consumption. A CFD study by T.D.Yuan reported that the heat transfer rates were improved by decreasing the area ratio around the heat sinks [6].While there are many studies available in the literature based on flow bypass [7]- [8], there are a very few which considers flow bypass along with thermal shadowing effect. Therefore this work focuses on improving the ducting system of the server with a view to achieve improved air delivery path in a server which is subjected to significant thermal shadowing. The main objective of this study is to reduce the cooling power consumption and flow rate required by the server to cool the components. This work involves both experimental and computational study to establish the case that the improved duct saves cooling power consumptions and flow rates by reducing the flow bypass. The study is further extrapolated to facility level analysis of traditional datacenter and highly efficient datacenter working on air side economization and the savings achieved at this facility level is presented

CHAPTER 2

Description of the server under study

2.1 Server description

The system considered for the study is an Intel based Open Compute server [9] which houses two microprocessors having thermal design power (TDP) of 95W each. CPU 0 thermally shadows CPU1 as seen in Figure 2.1. The server has a form factor of 2OpenU with cross-sectional area of 171mm x 807 mm. There are a total of 16 DIMM sticks available with a memory capacity of 8GB each. A cover is provided to the top of the server which directs the air flow inside the server.

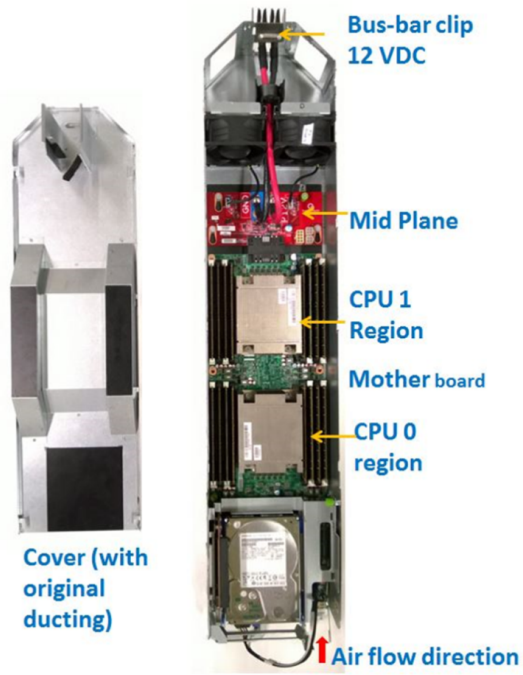

Figure 2.1. Open compute Server.

There are two fans provided at the rear end of the server to pull the air from the inlet to outlet of the server.The dimensions of the fans are 80mm x 80mm x 38mm. The speed of the fans are controlled by CPU die temperatures with the help of inbuilt fan control algorithms.These algorithms have a set target die temperatures, based on which the PWM signals control the fan speeds to draw required amount of air to cool the CPUs and heat sinks. The PCH chip set on the motherboard has a power consumption of 8W. A mid plane is provisioned at the rear end of the server which is responsible for connections between server fans, motherboard and the input power supply.

2.1.1 Ducting System of the server

The server is provided with removable chassis cover to which an air ducting system is integrated to direct the flow to components on the mother board. However, the ducting is provided only in the CPU1 region causing excessive flow bypass in CPU0 regions as shown in Figure 2.2. As a result, reducing the flow bypass by improving the ducting can lead to improved heat transfer and in turn reduce the burden on server fans. The detailed dimensions of the duct is shown in figure

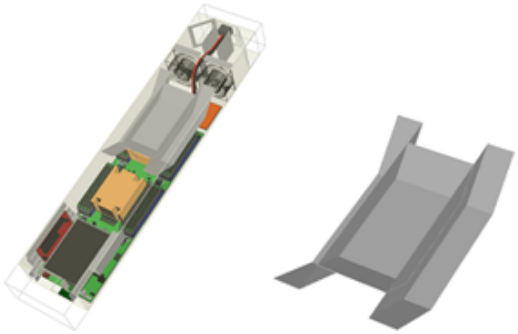

Figure 2.2. CFD model representing duct in CPU 1 region.

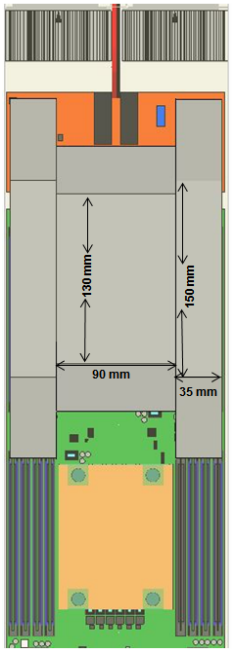

Figure 2.3. Top view of the chassis duct.

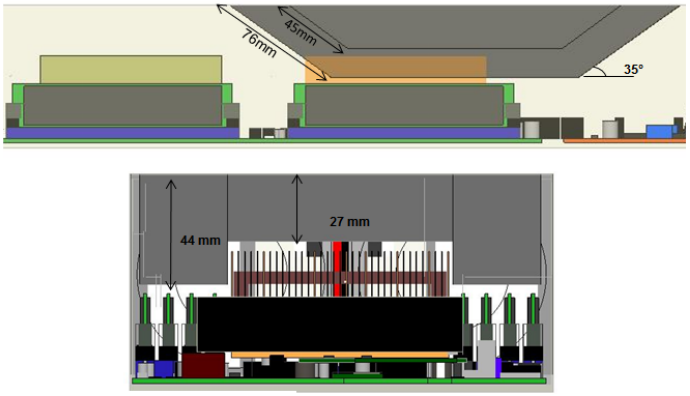

Figure 2.4. Side view and front view representing the dimensions of the duct.

CHAPTER 3

Experimental Characterization of the Baseline system

3.1 Flow Characterization of the Base Line Server

This section discusses about the experimental analysis of the baseline server to obtain the characteristic curves of the server and the server fans. Experiments such as system resistance curve, flow rate vs. duty cycle curve, fan curves and thermal tests are conducted at an ambient temperature of 24.5°C according to ASHRAE set limits [10]. Three trial runs are conducted to ensure for repeatability and consistency of the results.

3.1.1 Airflow Bench Test set Up

In order to evaluate the flow performance of the server, an airflow bench is employed [11]. Since the cross sectional area of the server ($171mm \times 88mm$) is way too less compared to the circular area of the airflow bench (36" diameter), a wind tunnel is constructed with exact cross section of the server and is attached to the rear end of the airflow bench as shown in the Figure 3.1. Tunnel length offset of 250mm from the inlet and outlet of the server is provided to avoid the effect of veena contracta caused due to sudden change in cross section from the airflow bench to the wind tunnel .The pressure taps are placed at a distance of 1 inch from the inlet and outlet of server. These taps are connected to pressure transducers on the airflow bench and the pressure readings are data logged in data acquisition software at the workstation.

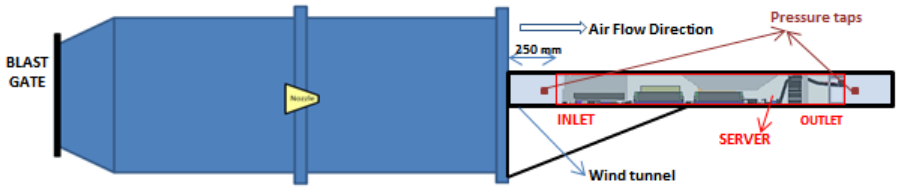

Figure 3.1. Representation of experimental setup on airflow bench.

3.1.2 System Resistance Curve

The server is fully populated with various heat generating and flow impeding components like heat sinks, DIMM sticks, CPUs, hard drives, capacitors and various VRDs. All these components obstruct the flow as air is passed through the server, and leads to the drop in pressure and the flow rate across the server. A system resistance curve is a curve of static pressure plotted with respect to flow rate across the server. It signifies the resistance offered by the server with varying flow rates. This curve is obtained by testing the server on an air flow bench with the nozzles facing in the downstream direction. The speed of the blower and the corresponding nozzle diameters are choose accordingly to achieve flow rates in the range of 0 to 150CFM (cubic feet per minute). Since the system resistance curve characterizes the system alone and not the fans, the fans are uninstalled. With the help of the pressure transducers, an average of 30 static pressure readings is noted down at the workstation at every flow rate supplied to the server. The experimental test results for system resistance curve are shown in figure and in Table 3.1.

3.1.3 Flow rate through the server

Fans are reinstalled and flow rate across the server is evaluated at various fan speeds which is controlled by varying pulse width modulation signal with the help of a function generator. Duty cycle (PWM signal) is varied from 0 to 100% and corre-

Table 3.1. Pressure drop values for various flow rates for the baseline server

Flowrate(cfm)	Static pressure(in/H_2O)
0	0
20	0.033
40	0.105
60	0.214
75	0.322
80	0.363
100	0.549
120	0.774
140	1.037
150	1.183

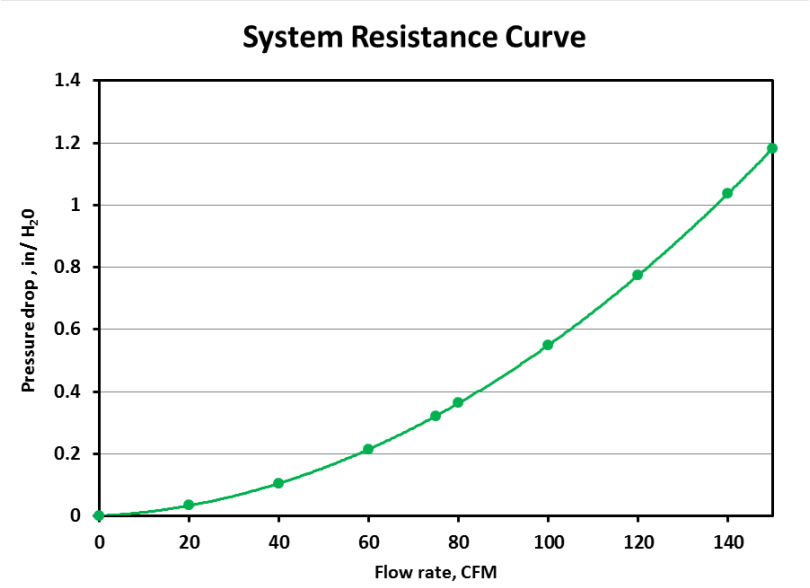

Figure 3.2. System resistance curve for baseline study.

sponding flow rate values and fan speeds in RPM's are noted down at the workstation. A curve of flow rate vs. duty cycle (PWM) and flow rate vs. RPM is plotted as shown in Figure 3.3 and in Figure 3.4respectively. The maximum flow rate achieved at 100% PWM is 120CFM. Table 3.2 contains the experimental test results of flow rates at various fan speeds.

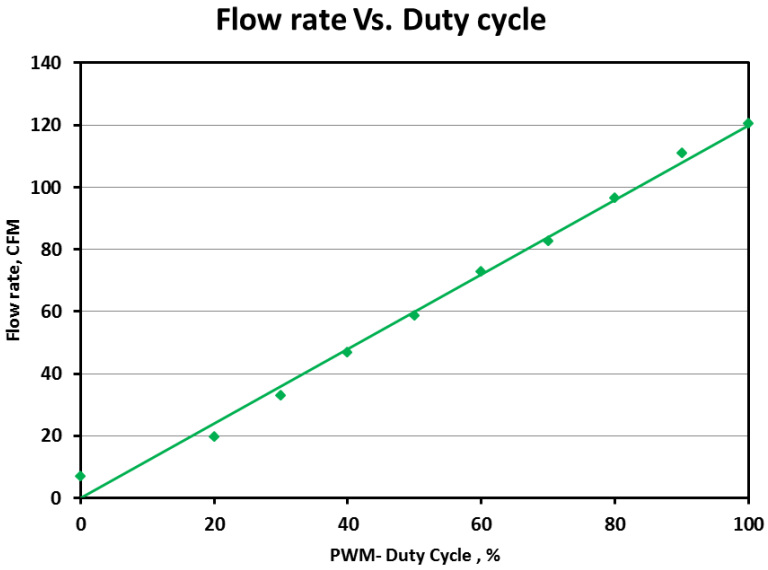

Figure 3.3. Flow rate vs. duty cycle for the baseline study.

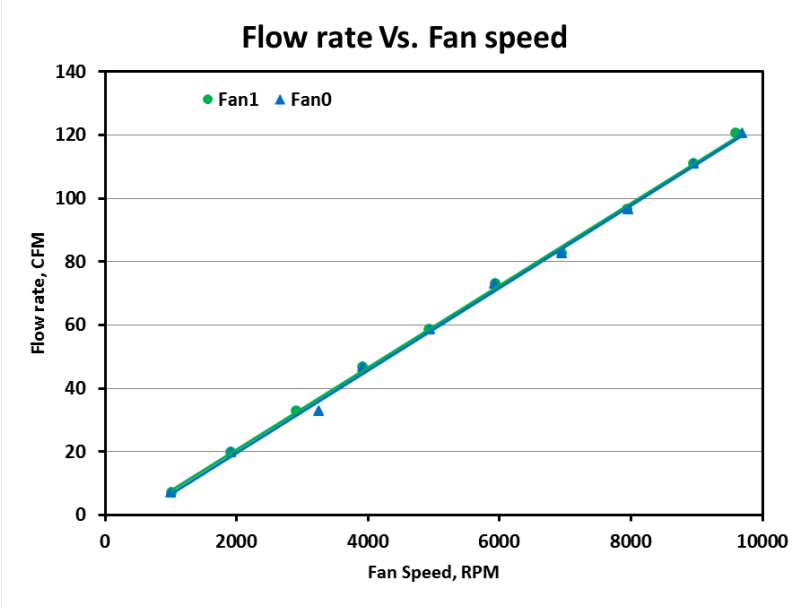

Figure 3.4. Flow rate vs. fan speed for the baseline study.

Table 3.2. Flow rate across the baseline server for various fan speed and PWM signals

Duty cycle	Flow rate	Fan 1 Speed	Fan 0 Speed
PWM%	CFM	RPM	RPM
100	120.39	9600	9705
90	110.82	8962	8966
80	96.47	7947	7968
70	82.67	6947	6965
60	72.92	5941	5947
50	58.59	4933	4961
40	46.71	3925	3933
30	32.81	2914	3267
20	19.73	1911	1926
0	7.06	1010	1009

3.1.4 Fan Performance Characteristics

A fan performance curve is of vital importance as it characterizes the capacity of the fan to push air with respect to the resistance offered. It is plotted with static pressure on y axis and flow rate on x axis. Two Sunon 80mm x 38mm (PF80381B1-Q020-S99) units are tested on the airflow bench to obtain the fan curves at 100% PWM. The test is conducted from full flow condition to no flow condition by gradually closing the blast gate and by selecting appropriate nozzles to achieve respective flow rates. The maximum static pressure and flow rate obtained is around 1.9in/H_2O and 100CFM.Table 3.3 contains the experimental test results of static pressures at various flow rates.

3.2 Thermal and Power Characterization of the Base Line server

Thermal experiments are conducted on the baseline server to evaluate the die temperatures, DIMM temperatures, fan speeds and the total power consumption of the server. In order to evaluate the power consumed by the fans, fans are powered externally and the power consumption is measured using LabVIEW. The experiment is

Table 3.3. Performance results for Sunon PF80381B1-Q020-S99

Flow rate(cfm)	Static Pressure(in/H_2O)
0.0	1.88
12.0	1.65
23.9	1.43
36.1	1.23
47.8	1.06
60.0	0.93
72.7	0.72
83.7	0.42
95.3	0.09
98.1	0.00

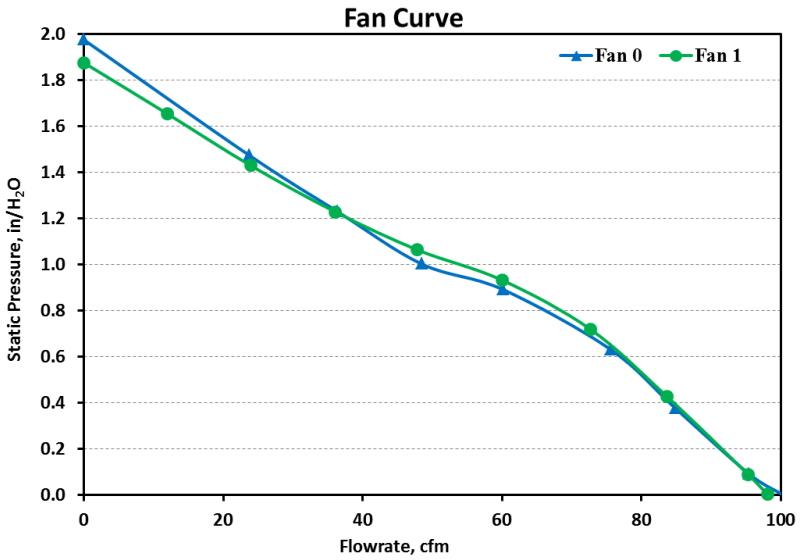

Figure 3.5. Fan Characteristic curve for Sunon.

conducted at an ambient temperature of 24.5°C according to ASHRAE set standards. An USB data logger is utilized to measure the surrounding temperature and the relative humidity. The test is conducted at various CPU power levels such as idle, 40%, 60%, 80% and 100% and at CPU+MEM where both the CPU and memory units are stressed simultaneously. It should be noted that at this condition CPUs are stressed lower than 100% stress level. Intels PTU tools are used to measure and load the CPU

and the memory units. Three test runs are conducted to ensure for repeatability and consistency. Tests are conducted for 18 hours involving 3 trial runs of 6 hours each to ensure for repeatability. Average of readings at last ten minutes, at each power level is noted to account for accurate measurements after the fans have reached the stable condition.Table 3.4 contains the experimental test results at various power levels.

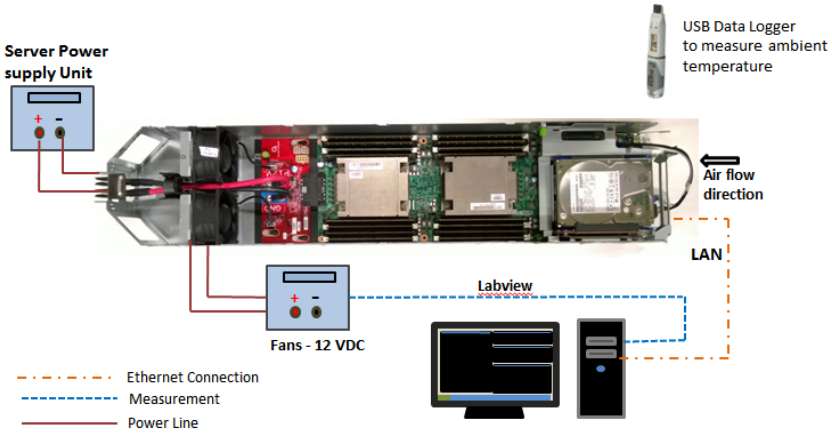

Figure 3.6. Representation of the test set-up - Thermal characterization.

Table 3.4. Experimental results for thermal characterization of baseline server

Power Levels(%)	Ambient T $^{\circ}C$	CPU 0 Die T°C	CPU 1 Die T°C	Server Power(W)	Fan Power(W)	Flow rate (CFM)
Idle	24.5	51.95	41.80	46.25	0.94	11.04
40%	24.5	73.44	55.83	132.66	1.74	24.3
60%	24.5	73.70	58.97	156.23	2.21	30.12
80%	24.5	74.57	61.99	184.33	2.79	35.17
100%	24.5	73.78	63.83	210.87	3.87	43.37
CPU+MEM	24.5	73.44	60.34	188.74	2.62	33.44

It can be seen that in Figure 3.7 the power consumed by the server is increasing from idle to 100% CPU stress level, where as the power consumption drops at MEM+CPU condition , due to the reason that the CPUs are stressed lower than at 100% power level. Similar trend can be observed in all the experimental results shown through out from Figure 3.8

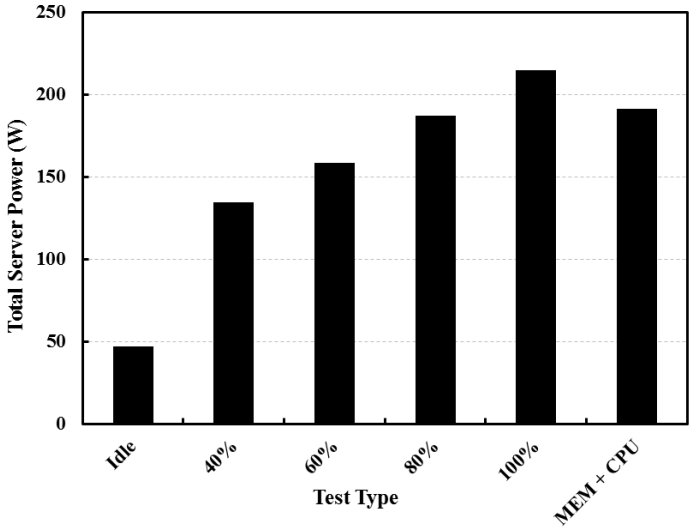

Figure 3.7. Total server power of the baseline server at various power levels.

Fan speeds vs power levels is represented in Figure 3.9, where the maximum speed per fan is 3750 rpm at 100% CPU power level with power consumption of 3.87W consumed by both the fans and the minimum speed per fan being 975 rpm at idle condition with both the fans consuming 0.94 W. Figure 3.10 represents average CPU die temperatures at various power levels. It is observed that the average CPU0 temperatures are around 73°C to 75°C and average CPU1 temperatures are around 55°C to 63°C from 40% to MEM+CPU condition.However the CPU temperatures are lower at idle condition i.e. the average CPU temperatures of CPU0 and CPU1 are 52°C and 42°C respectively. In all these power levels it can be observed that

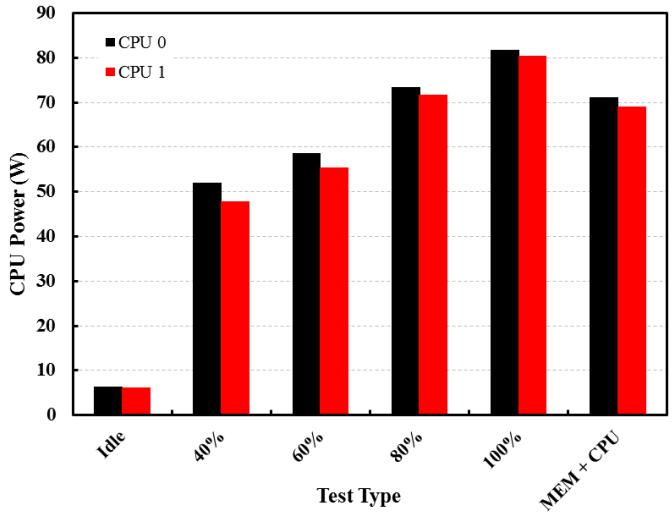

Figure 3.8. CPU power consumption at various power levels.

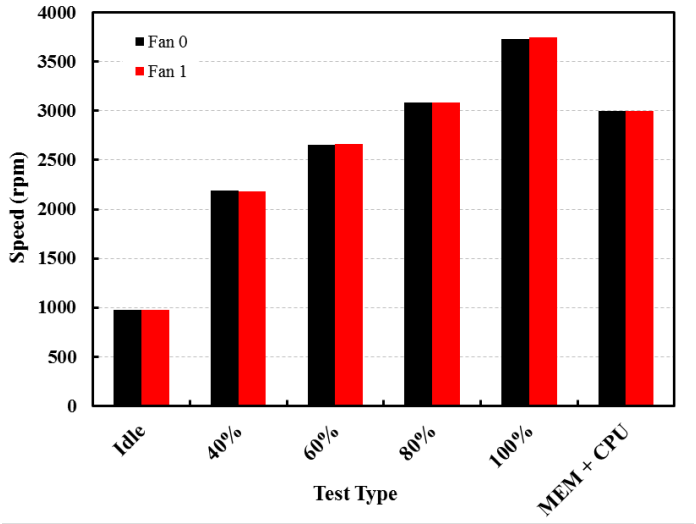

Figure 3.9. Fan speeds at various power levels.

CPU 1 temperatures are comparatively lower than CPU0 temperatures due to the fact that the ducting is provided only for CPU1 region, resulting in over cooling of CPU1 temperatures. Figure 3.11 shows the fan power consumption at various power levels. The fan power consumption continues to increase as the CPU stress levels are increased from IDLE to 100% and at CPU+MEM it consumes comparatively lesser

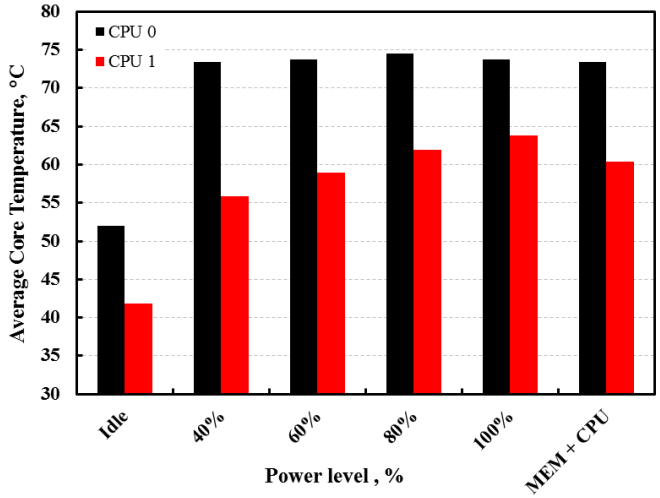

Figure 3.10. Average CPU die temperatures at various power level.

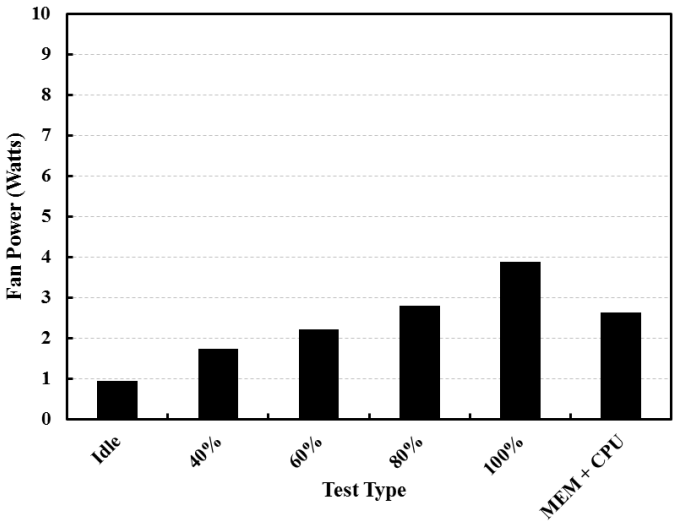

Figure 3.11. Fan power in watts at various power level.

power than 100% power level. As the load on the CPUs increases, the fan speed is also correspondingly increased to maintain the CPUs at the recommended target die temperatures.

CHAPTER 4

Computational Fluid Dynamics (CFD) for baseline study

4.1 Detailed CFD model of Open Compute server

This chapter discusses about the methodology followed to calibrate a CFD model with experimental test results. Calibration of a CFD model is essential to parametrically improve the duct in the server . A detailed CFD model is generated in 6SigmaET, which is a commercially available CFD code with nomenclature identical to those used in electronics industry [12]. The server is modeled with all heat generating and flow impeding components including CPUs, heat sinks, DIMMs, chipsets , server fans and various mosfets , VRDs and chokes and is solved using K-E turbulence model. Temperature of 24.5°C is specified as the inlet temperature to the server. Basically the CFD modeling is divided into flow modeling and thermal modeling

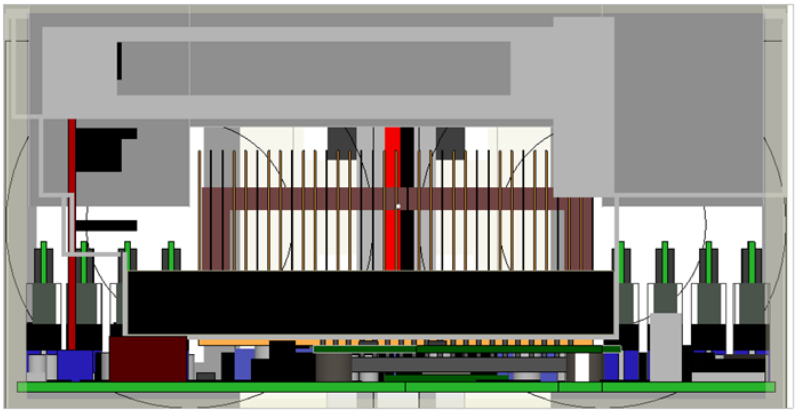

Figure 4.1. Front view of the server model.

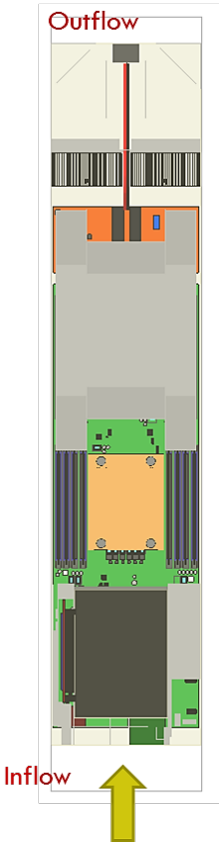

Figure 4.2. Top view of the server model.

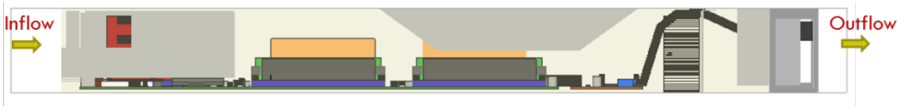

Figure 4.3. Side view of the server model.

4.2 Mesh sensitivity analysis

4.2.1 Mesh sensitivity analysis with fans uninstalled

Mesh Sensitivity analysis is performed to ensure that the solution is independent of the grid counts. Since the evaluation of system resistance does not involve the fans, sensitivity analysis is performed by uninstalling the fans and is simulated at 3, 6, 12, 24 and 48 million cells. 75 CFM is prescribed at the front end of the chassis and the rear end is opened to the environment. The termination factor is set to 0.1 to

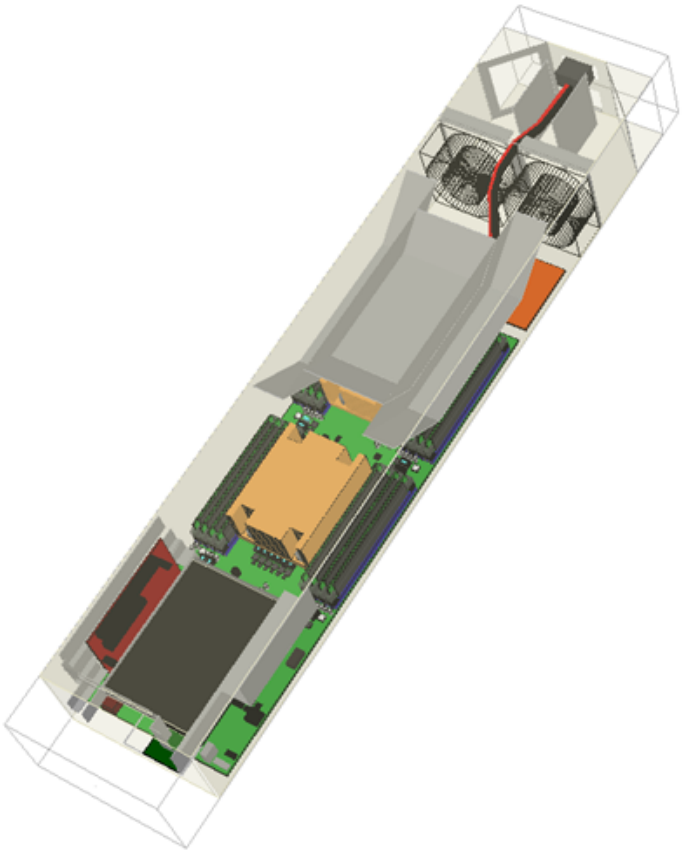

Figure 4.4. Isometric view of the detailed server model.

ensure accurate solution. It is observed that the model becomes grid independent at 24 million cells as shown in Figure 4.5

4.2.2 Mesh sensitivity analysis with fans installed

The Mesh Sensitivity analysis is performed again to ensure the independence of results when the fans are installed back to estimate flow rates and component die temperatures inside the server. Both the front and the rear vents of the chassis is open to environment and the flow through the server is achieved with the help of server fans. Sensitivity analysis is performed at 3, 6, 12, 24 and 48 million and is

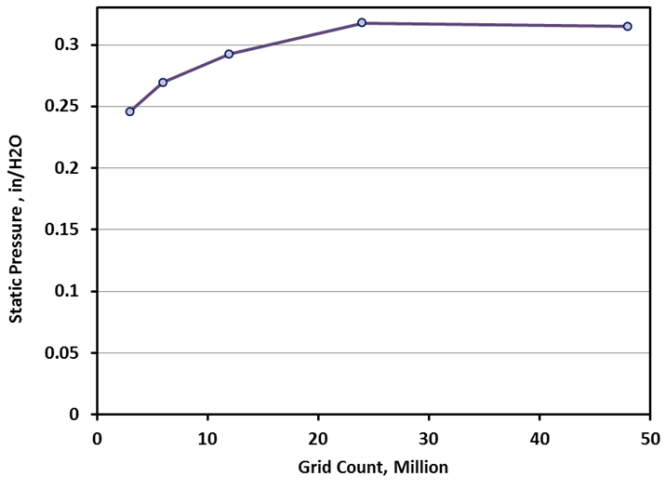

Figure 4.5. Grid independence study of static pressure.

observed to be grid independent at 24 million cells as well as shown in Figure 4.6. The termination factor is set to 0,01 and the appropriate device relaxation factors are specified to the fans. Figure 4.6 shows the grid independence in terms of CPU Die temperatures

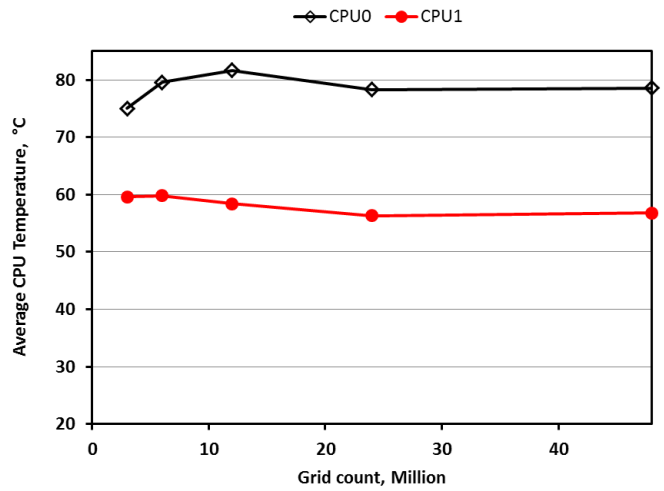

Figure 4.6. Grid independence study of average CPU die temperatures.

4.3 Flow analysis using CFD

4.3.1 System resistance curve using CFD analysis

Beginning from this section to the end of this chapter, comparison between CFD and experimental test results are made for the baseline server. Specific flow rates are specified at the inlet of the grid independent model and corresponding static pressure readings are noted down to plot a curve of static pressure Vs. Flow rate which is termed at System Resistance Curve. Figure shows the comparison of System resistance curve obtained through experimental and numerical model. It can be seen in Table 4.1 that the system resistance curve obtained computationally is in excellent agreement with the experimental results(within 8% error)

Table 4.1. Comparison of pressure drop between numerical and experimental test results

	System Pressure drop		
Flow rate(cfm)	Experimental	CFD	Error %
20	0.033	0.034	1.3%
40	0.105	0.106	1.6%
60	0.214	0.214	-0.3%
75	0.322	0.318	-1.3%
100	0.549	0.522	-5.0%
120	0.774	0.714	-7.7%

4.3.2 Flow rate through the server at various duty cycle

Using the correlation between fan speeds (RPM) and duty cycle (%) as seen in Table 3.2, fan speeds in rpm is specified to the model and corresponding flow rates across the server is noted down. Table 4.2 shows the percentage error between experimentally and numerically obtained flow rates and it can be observed that the

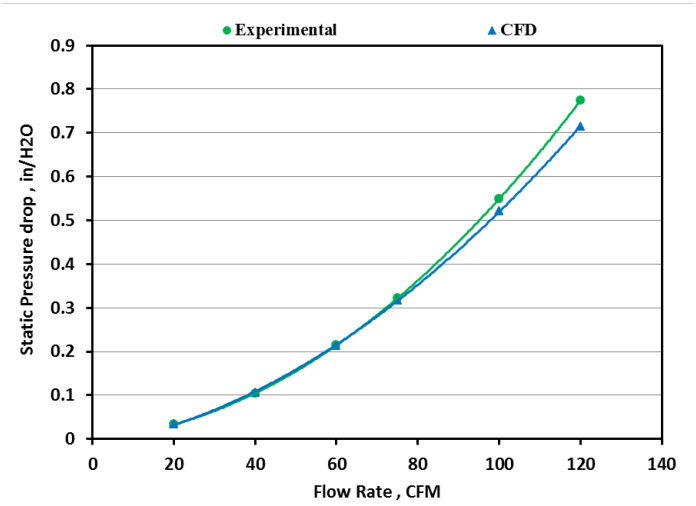

Figure 4.7. Comparison of experimental and numerical system resistance curve.

flow model is validated with error less than 8%. Figure shows the comparison between them.

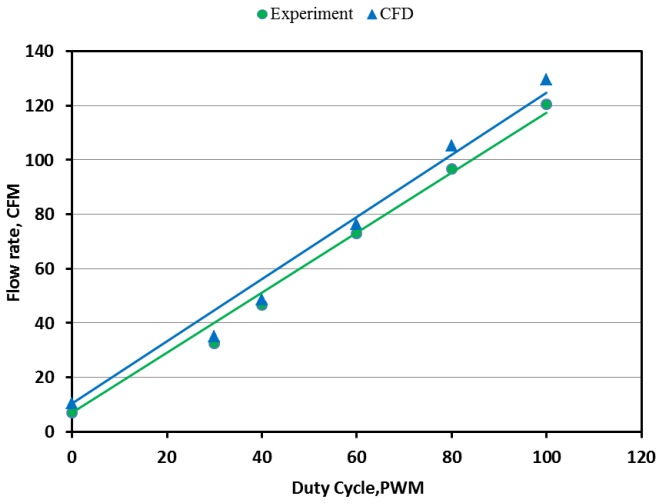

Figure 4.8. Plot comparing experimental and computational flow rates .

Table 4.2. Comparison between experimental and computational flow rates

	Flowrate(cfm)		
PWM%	Experimental	CFD	Error %
100	120.4	129.6	7.1%
80	96.6	105.3	8.2%
60	72.9	76.5	4.7%
40	46.7	48.7	4.1%
30	32.6	35.1	7.3%
0	7.1	10.5	32.5%

4.4 Thermal analysis using CFD

Inlet temperature of 24.5°C is specified as the environmental temperature. Experimentally obtained component power consumptions and fan speeds at various power levels, are used as inputs to the CFD model. Due to the lack of knowledge on accurate thermal conductivities of various components, the model is calibrated by assigning appropriate thermal conductivities to match the experimental temperatures of the components [13]. From Table 4.3 it can be seen that the thermal model is calibrated with an error of less than 14.5%.

Table 4.3. Comparison of CPU 0 die temperatures obtained by experimental and numerical methods

	CPU 0 Die temperature		
Power level%	Experimental	CFD	Error %
Idle	45.5	51.95	14.18%
40%	74.18	75.7	2.05%
60%	74	72.5	-2.03%
80%	73.73	76	3.08%
100%	73.66	74.6	1.28%
CPU+MEM	74.56	78.5	5.28%

CHAPTER 5

Improving the Ducting system of the Server

5.1 Parametrically improving the duct using CFD analysis

The calibrated CFD model is used to simulate various duct designs to aid the understanding of the flow distribution inside the server. Supplying sufficient flow to all the critical components such as CPUs and DIMMs, are an important aspect in air flow management. As discussed in chapter 2, the duct on the chassis body is provided only in CPU 1 region resulting in majority of the cold air bypass through the upstream region (CPU 0 region), leading to increase in CPU 0 temperatures which controls the fan speeds through inbuilt fan control algorithm. It is also of vital importance to consider the effects of thermal shadowing due to the mixing of hot and cold air behind CPU1 as can be seen in Figure 1.3. Excessive reduction in bypass in the upstream region might result in rise of CPU1 temperatures which in turn will lead to rise in total server power consumption as well. Therefore an optimal balance has to be maintained between the two The fan speeds and power measurements obtained at CPU+MEM condition during baseline experimental study is used as inputs to the model.A set of designs are generated and studied for nature of flow through the heat sinks and Dimms by the use of result phases available in the CFD code. The goal of the parametric study is to reduce CPU 0 temperatures nearly equal to CPU 1 temperatures by decreasing the bypass area around the upstream heat sink. The tip clearance above the heat sink in downstream region(CPU 1 region) was 4mm in baseline study and in this process of parametrization the tip clearance in CPU 1 region is reduced to 2mm to avoid unwanted bypass in this region. And the duct in span

wise clearance area i.e. on top of the DIMMS are extended to cover the entire length of DIMMS. This is done to reduce the span wise clearance in upstream region(CPU 0 region) and also to increase the velocity of air passing through the DIMMS. A series of simulations are conducted to obtain appropriate angle to the span wise duct. Yet, since there were no changes observed in DIMM temperatures or CPU temperatures, 90 angle was selected to ease the process of prototyping. Maintaining these changes in the duct , further the study is continued by varying the tip clearance above heat sink 0 from 31mm(maximum tip clearance) , 26mm , 20mm and 17mm. It is observed that as the tip clearance is reducing , the CPU 0 temperaturesbegins to fall , however CPU 1 temperatures began to increase which in the real time system would lead to increase in CPU 1 power consumption which increases the server power consumption.Therefore, the best design is the one which has maximum tip clearance above heat sink 0, with the span wise clearance completely blocked. Detailed dimensions of improved is show from Figure5.1 to Figure5.5

5.2 Temperature and Velocity plots

Figure 5.6 represents the temperature plots of baseline and Improved duct designs obtained through CFD analysis.The result plots are recorded at an height of 43.5mm. It is evident from Figure 5.6 that, in improved duct case the heat sink temperatures are lower than in baseline scenario, which is due to better air flow distribution.

Figure 5.7 represents the velocity plots of both improved duct and baseline duct scnerios. It can be observed that the velocity of air is comparatively higher through the heat sinks and above the DIMMS in improved duct case.

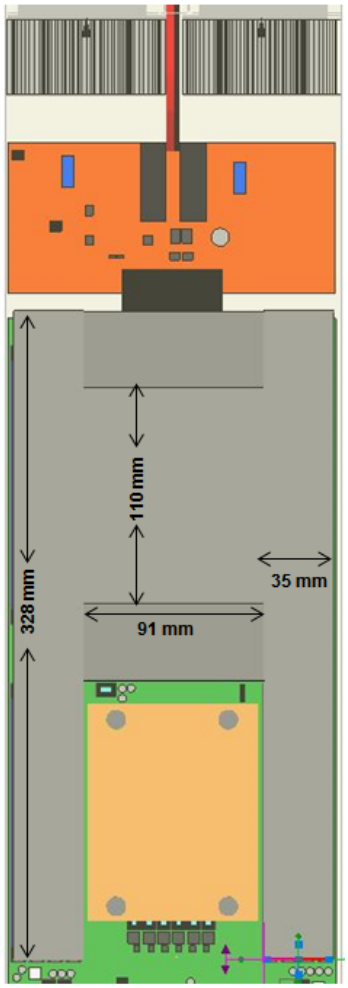

Figure 5.1. Top view of the server with improved duct design.

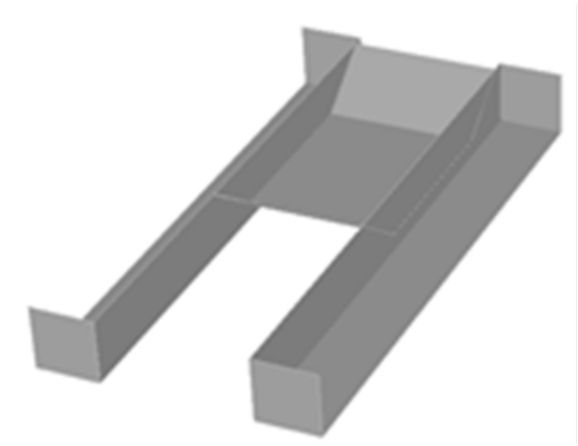

Figure 5.2. Mechanical structure of improved duct design.

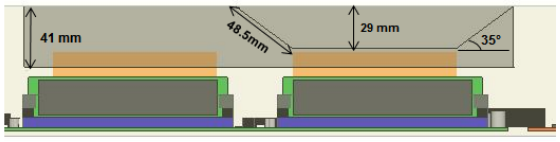

Figure 5.3. Side view of the server with improved duct design.

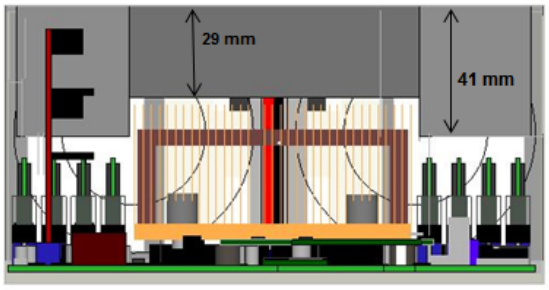

Figure 5.4. Front view of the server with improved duct design.

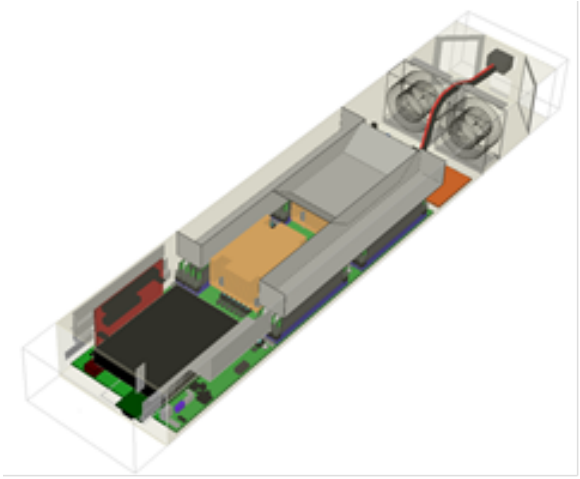

Figure 5.5. Isometric view of the server with improved duct design.

5.3 Prototyping the duct for experimental analysis

CFD analysis plays an important role leading to an understanding about the flow patterns inside the server, however the CPU die temperatures and DIMM temperature drawn by the model simulation is not used as an accurate solution to the problem due to the fact that the fan speeds and power inputs are fixed in the model,

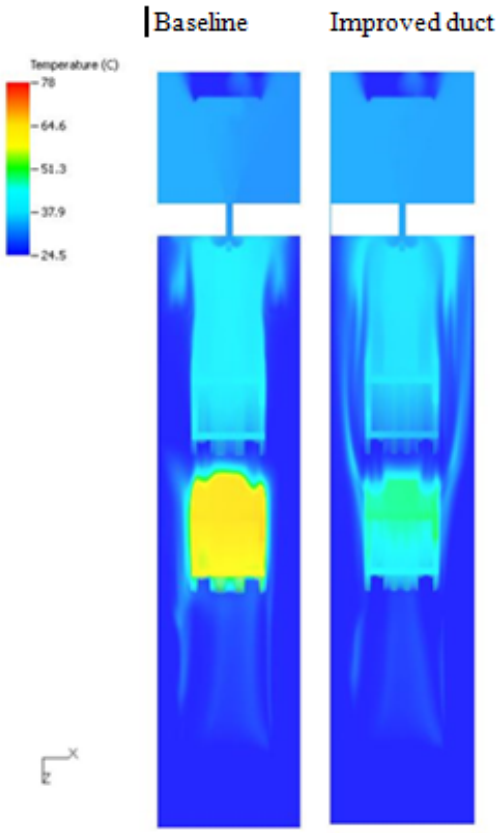

Figure 5.6. Temperature plots for baseline and improved duct designs .

where as in the datacenter the fan speeds are controlled by fan control algorithm which is mostly triggered by the CPU die temperatures in the servers.Therefore it becomes mandatory to verify the duct designs experimentally. Improved design is prototyped using acrylic sheets and tested experimentally to draw the CPU die temperatures , fan speeds, power consumed by fans, DIMM temperatures and Total server power consumption. Tests are conducted for 18 hours in the similar way followed in baseline experimental testing.The fans are powered externally to measure the power consumption using Labview at the workstation.

According to CFD analysis,the improved design was the one with tip clearance in CPU 0 region. In order to experimentally verify that reduction in tip clearance

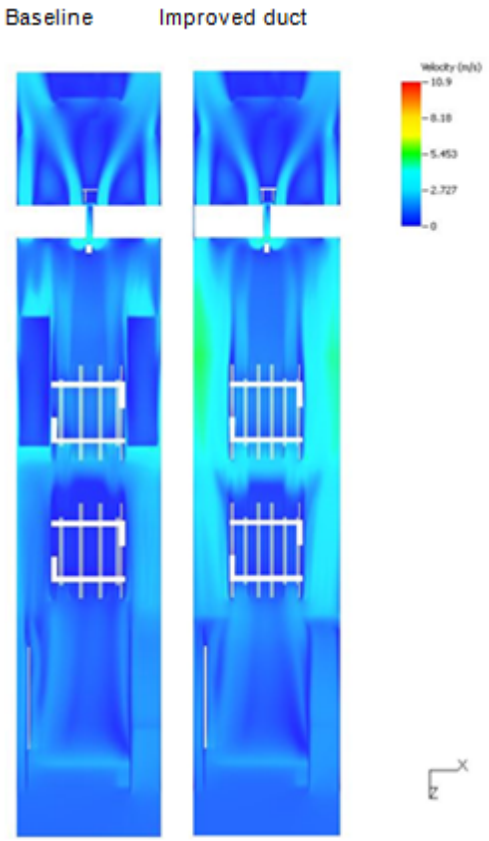

Figure 5.7. Velocity plots for baseline and improved duct designs.

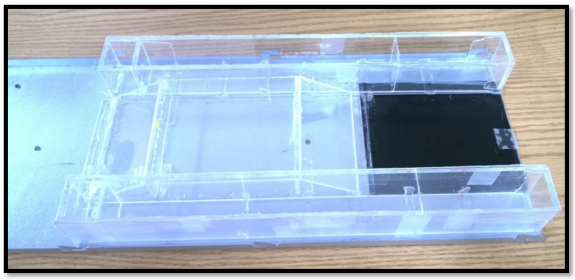

Figure 5.8. Improved duct prototyped using acrylic sheets.

Figure 5.9. Server with improved chassis duct.

would increase the CPU 1 power consumptions and temperatures, tip clearances were reduced by adding acrylic sheets in Region 1. It was observed that as the tip clearances are reduced, the IT power consumption started to increase. Therefore it is evident that the design that has maximum tip clearance in Region 1 is the optimum design as the IT power consumption remains the same as the power consumption of the baseline server.

CHAPTER 6

Results and Discussion

6.1 Comparison between baseline and Improved duct scenarios

This chapter presents the discussion on the results and savings obtained by improving the duct design of the server and testing it experimentally.

6.1.1 IT power consumption

IT power consumption includes only the server power consumption and excludes the fan power as the fans are powered and masured externally.It was noticed that the IT power consumption is the same in both the duct design scenarios as seen in Figure 6.1. Both the servers have a maximum IT power consumption of around 211W. Having this fixed, savings in fan power consumption is observed.

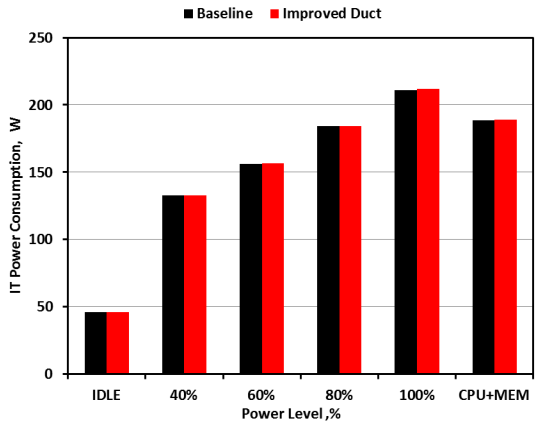

Figure 6.1. IT power consumption for the baseline and improved duct designs.

6.1.2 Savings achieved in fan power consumption

Figure 6.2 indicates the fan power consumption in both the duct design scenarios. As the CPUs are stressed from idle to 100% the fan power increases gradually. The fan power consumption is lower at CPU+MEM than at 100% CPU stress level because at this condition the CPUs are powered lower than 100%. As a result of improved duct , 23.4%-40% savings in power consumed by the fan is achieved as the CPU stress level is increased from 40% to 100% and 31% savings is observed at CPU+MEM. Even though there are no savings achieved at the idle state, there are no losses in the cooling power consumption which makes it possible to implement the improved design even to the servers which are idling most of the times.Table 6.1 represents the savings achieved in fan power consumption.

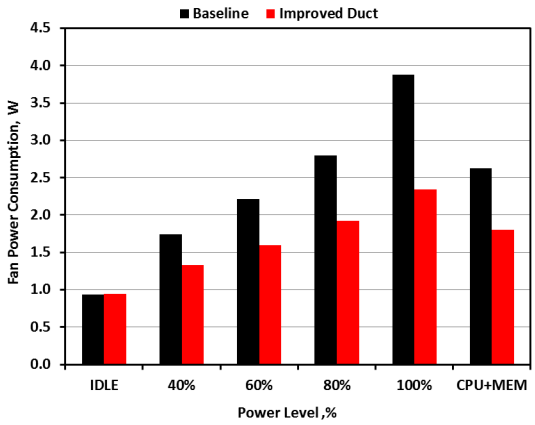

Figure 6.2. Fan power consumptions for the baseline and improved duct designs.

6.1.3 Savings achieved in fan speed

Due to improved air distribution pattern inside the server, the server requires lesser flow compared to baseline to cool the CPUs and to maintain them within the recommended limits. Figure 6.3 represents the reduction in fan speeds is observed in

Table 6.1. Fan power consumptions for baseline and improved duct designs

	Fan Power Consumption in Watts		
Power level%	Baseline	Improved Duct	Savings %
Idle	0.94	0.94	0%
40%	1.74	1.33	-23%
60%	2.21	1.59	-28%
80%	2.79	1.93	-31%
100%	3.87	2.34	-40%
CPU+MEM	2.62	1.80	-31%

the improved duct server. Similar to a trend seen in cooling power consumption, the fan speeds starts to ramp up as the CPUs are stressed from idle to 100%. Fan speed is lower at CPU+MEM than at 100% CPU power level due to the fact discussed earlier. 22%-26% reduction in fan speed is seen in improved duct case when CPUs are stressed from idle to 100% and 23.7% reduction in fan speed is observed at CPU+MEM. Similar to total server power consumption and cooling power consumption, there is no change in fan speed at idle case. Reduction in fan speeds results in minimizing the flow rates through the server and in fan acoustic levels which will be discussed in the further sections. Table 6.2 represents the reduction in fan speeds achieved.

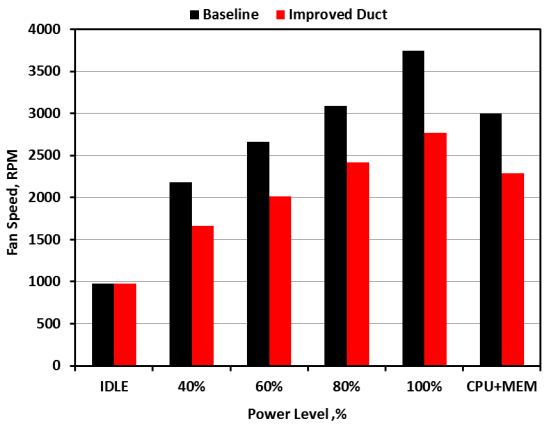

Figure 6.3. Fan speeds for baseline and improved duct designs.

Table 6.2. Fan speeds for baseline and improved duct designs

	Fan Speeds in RPM		
Power level%	Baseline	Improved Duct	Savings %
Idle	975	975	0%
40%	2183	1660	-24%
60%	2659	2012	-24%
80%	3085	2417	-22%
100%	3741	2767	-26%
CPU+MEM	2999	2287	-24%

6.1.4 System resistance curve for the baseline and improved duct designs

To estimate the system resistance curve for both the duct design scenarios, the servers were mount on the rear end of the airflow bench and tested for estimating static pressure drop readings at various flow rates. A slightly higher static pressure is observed in improved duct server, however the savings achieved in flow rate and fan power consumption compensates the pressure drop loss. Figure 6.4 represents the system resistance curve for various flow rates.

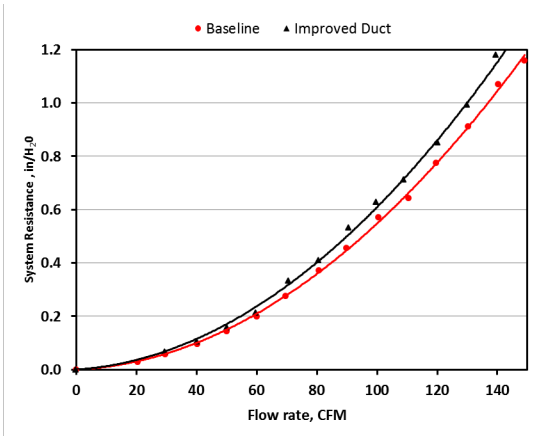

Figure 6.4. System resistance curve for baseline and improved duct designs.

6.1.5 Reduction in flow rates required by the server

Due to reduction in fan speeds, the flow rates required by the server decreases. In order to estimate the flow rates required by both the servers , an airflow bench is employed. Fans are controlled and powered externally. Fan speeds corresponding to various utilization is replicated while the experimental testing and the corresponding flow rates are measured from the workstation. Figure 6.5 shows the flow rates across improved and baseline duct scenarios at various CPU stress levels and at CPU+MEM. 31.3%-37.3% reduction in flow rates is achieved as a result of reduced fan speeds. However even due to the reduction in flow rates, there is no detrimental increase in CPU power consumptions. Table 6.3 shows the savings achieved in flow rates across the server.

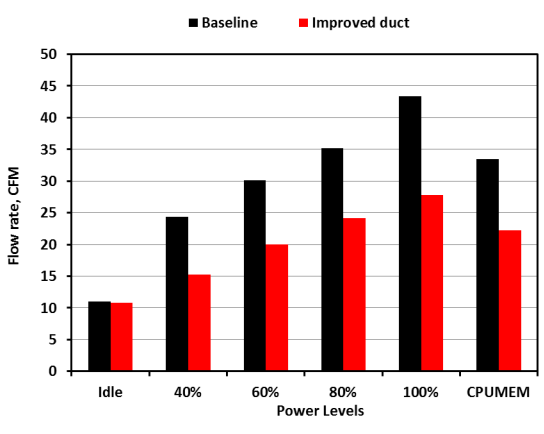

Figure 6.5. Flow rates across baseline and improved duct designs.

Figure 6.6 represents the average CPU 0 die temperatures at various CPU power levels and at CPU+MEM.It can be seen that the average CPU 0 die temperatures are around 74C in both the duct designs. Therefore it is verified that the CPU die temperatures do not increase with the reduction in flow rates across the server

Table 6.3. Flow rates across the baseline and improved duct designs

	Flowrates in cfm		
Power level%	Baseline	Improved Duct	Savings %
Idle	11.04	10.81	2%
40%	24.32	15.25	37%
60%	30.12	20.05	33%
80%	35.17	24.16	31%
100%	43.37	27.816	36%
CPU+MEM	33.44	22.20	34%

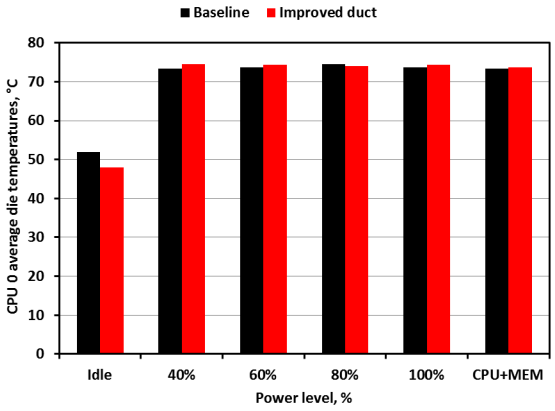

Figure 6.6. Average CPU 0 die temperatures for baseline duct and improved duct designs.

6.1.6 Reduction in acoustic noise levels of the server fans

This section discusses about the reduction in noise levels of the fans due to observed reduction in fan speeds. Noise is an important parameter to be reduced in a data center to facilitate noise free communications between workers in datacenter. Lowering the noise levels also removes the mental stress on the data center operators. Therefore it is of vital importance to take steps to reduce noise levels in data centers. According to OSHA, the sound pressure levels are not permitted to rise more than 90dB (A) for US and 85dB (A) for the European countries [14]. Noise tests are conducted to estimate the acoustic levels of fans at various CPU power levels and at

CPU+MEM. Fan noise levels in dB(A) are measured experimentally using an application software. The ambient noise level of the room is 40 dB(A). The microphone is positioned at a distance of 1m away from the fans(noise source) and the readings are recorded after letting the fan to stabilize for 10 minutes. Figure 6.7 shows the experimental test set up for measuring noise levels of server fans. Table 6.4 represents the reduction in acoustic noise levels.

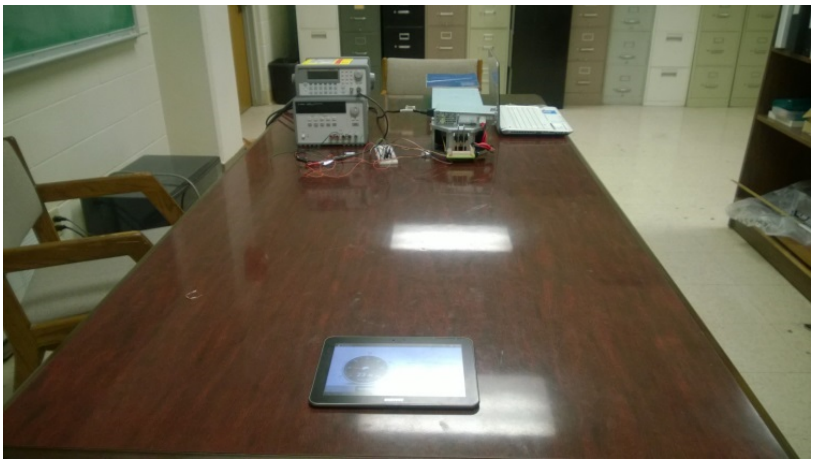

Figure 6.7. Experimental test set up for measuring noise levels.

Table 6.4. Flow rates across the baseline and improved duct designs

	Noise level (dB)		
Power level%	Baseline	Improved Duct	Savings %
Idle	43	43	0%
40%	47	44	6.4%
60%	50	45	10.0%
80%	55	47	14.5%
100%	60	50	16.7%
CPU+MEM	52	46	11.5%

It can be observed that 6.4% to 16.7% reduction in acoustic levels is obtained due to decreased fan speeds in improved duct scenario. There is no change in fan speed observed at idle condition, therefore there is no reduction observed in acoustic noise levels as well.

CHAPTER 7

Facility Level Analysis

An energy Logic model by Emerson Network Power reported that one Watt of power saved at the server level extrapolated to as much as 2.84 Watts at the facility level [4]. The savings achieved in this study at the server level is extrapolated to facility level analysis on traditional data center and highly efficient data center working on air side economization.

7.1 Traditional Datacenter.

IT power consumption includes only the server power consumption and excludes the fan power as the fans are powered and measured externally.It was noticed that the IT power consumption is the same in both the duct design scenarios as seen in figure 6.1. Both the servers have a maximum IT power consumption of around 211W. Having this fixed, savings in fan power consumption is observed.

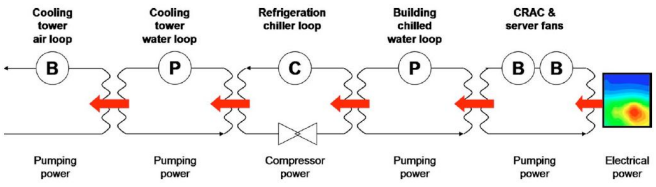

Figure 7.1. Cooling energy loop of a traditional datacenter.

In order to extrapolate the savings achieved at server level to a traditional datacenter facility, a physics based model presented by Iyengar and Schmidt is employed [15]. The model presents a set of equations that can be employed to calcuate

the total pumping power, flow rates , CRAC pumping power and number of CRAC units to be used in a datacenter room. The primary power consumption components are the server fans, CRAC Units, Building chilled water pumps, compressors, condensers and cooling tower blowers. All the input parameters considered in the physics based model is assumed identical to our study except the flow rates through building chilled water pumps, cooling tower air loop and water loop due to the fact that the physics based model did not have a set Ttile temperature, however out study requires a Ttile temperature of 24.5C, therefore Ttile temperature is set to 24.5C and back calculations are performed to estimate the flow rates across building chilled water pumps, cooling tower air loop and water loop. In our analysis 350 racks are assumed with 45 servers per rack , with a rack density of 9.6KW. It was observed that maximum pumping power of 1.35MW is needed to cool IT heat load of 4MW, in baseline scenario. Whereas in improved duct scenario 1.3MW of pumping power is required to cool an IT load of 3.7MW. Thereby savings are achieved in total pumping power as seen in Table 7.1. Due to reduction in flow rates in improved duct server, the total reduction in flowrates across the entire datacenter reduces leading to reduction in number of CRAC units required to cool a datacenter room, as presented in Table 7.4. 10-19 CRAC Units can be shut-off which leads to reduced CRAC Power consumption as seen in Table 7.2. Maintenance costs are also reduced by reducing the number of CRAC Units

7.2 Highly efficient datacenter working on airside economization

7.2.1 Savings in fan wall power consumption

Figure 7.4 represents highly efficient datacenter design layout working on airside economization. Bringing in outside air directly to the datacenter as a primary source

Parameter Description	Symbol	Value
Electromechanical Efficiency of CRAC	η_{CRAC}	0.5
Electromechanical efficeincy of building chilled water pump	η_{BCW}	0.8
Electromechanical efficeincy of cooling tower pump	η_{CTW}	0.8
Electromechanical efficeincy of cooling tower fans	η_{CTA}	0.8
Pressure loss coefficient for rack front door	C_{fd}	3 $Pa^{0.5}$ / (m^3/s)
Pressure loss coefficient for rack rear door	C_{rd}	3 $Pa^{0.5}$ / (m^3/s)
Pressure loss coefficient for CRAC internals	$C_{CRAC,int}$	3.55 $Pa^{0.5}$ / (m^3/s)
Pressure loss coefficientfor the building chilled water loop	C_{BCW}	1557 $Pa^{0.5}$ / (m^3/s)
Pressure loss coefficientfor the cooling tower water loop	C_{CTW}	1311 $Pa^{0.5}$ / (m^3/s)
Pressure loss coefficientfor the cooling tower air path	C_{CTA}	0.12 $Pa^{0.5}$ / (m^3/s)
Fraction of the total building chilled water heat load in data center	γ_{BCW}	1
Fraction of the total rack flow, which bypasses the server nodes	ϕ_{rack}	0
Fraction of total rack flow rate that is supplied by the tiles	δ_{supply}	0.555
Fraction of the total data center flow rate attributed to leakage	$\delta_{leakage}$	0.5
Factor of flow overprovisioning	$\beta_{over\ Provision}$	1
Factor to account for under floor and tile pressure drop	β_{CRAC}	0.2
Fraction of building chilled water that is routed to the data center	δ_{BCW}	1
No. of microprocessor modules in parallel in the node N module	$N_{module,p}$	2
No. of microprocessor modules in series in the node N module	$N_{module,s}$	1
No. of server nodes in the rack N node	N_{node}	45
No. of racks in the data center N rack	N_{rack}	350
Chilled water set point temperature at chiller evaporator exit	T_{cho}	280 K
Thermal conductance of the CRAC unit heat exchanger coil	UA_{CRAC}	23,000 W/K
Dew point of the air entering the cooling tower		20 °C
Relative humidity of the air entering the cooling tower		0.88
Atmospheric pressure at the inlet of the cooling tower		101.3 Kpa
Cooling tower parameter	c	2
Cooling tower parameter	n	0.6
Specific heat of air Cp air	Cp_{air}	1007 J/Kg K
Mass density of air	ρ_{air}	1.16 Kg/m3
Specific heat of water Cp water	Cp_{water}	4179 J/Kg K
Mass density of water	ρ_{water}	995 Kg/m^3

Figure 7.2. Input parameters considered for the analysis.

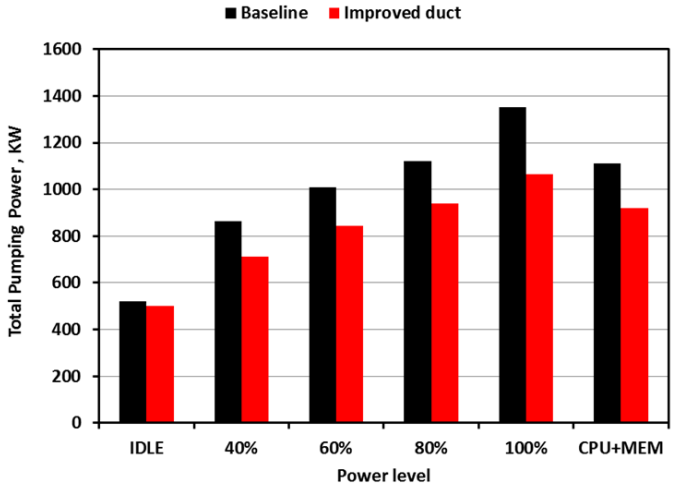

Figure 7.3. Savings achieved in total pumping power.

Table 7.1. Savings achieved in Total pumping power

	Total Pumping Power in KW		
Power level%	Baseline	Improved Duct	Savings %
Idle	520.08	499.66	3.9%
40%	864.93	713.35	17.5%
60%	1007.46	843.85	16.2%
80%	1119.82	939.32	16.1%
100%	1352.13	1066.41	21.1%
CPU+MEM	1111.91	919.72	17.3%

Table 7.2. Savings achied in CRAC Pumpimg power

	CRAC Pumping Power in KW		
Power level%	Baseline	Improved Duct	Savings %
Idle	165.68	165.68	0%
40%	364.98	228.86	37.3%
60%	452.02	300.90	33.4%
80%	527.81	362.58	31.3%
100%	650.87	417.45	35.9%
CPU+MEM	501.70	333.26	33.6%

Table 7.3. Savings achieved in Total pumping power

	Total Pumping Power in KW		
Power level%	Baseline	Improved Duct	Savings %
Idle	520.08	499.66	3.9%
40%	864.93	713.35	17.5%
60%	1007.46	843.85	16.2%
80%	1119.82	939.32	16.1%
100%	1352.13	1066.41	21.1%
CPU+MEM	1111.91	919.72	17.3%

of cooling eliminates the use of compressors and chillers leading to high performance of datacenters.

Outside air is bought into the datacenter through the inlet louvers and is sent to the filter bank directly or by mixing it with the return air to rise the air tem-

Table 7.4. Savings in CRAC Units

	Number of CRACs Units Saved		
Power level%	Baseline	Improved Duct	Savings %
Idle	13	13	0
40%	28	18	10
60%	35	23	12
80%	41	28	13
100%	51	32	19
CPU+MEM	39	26	13

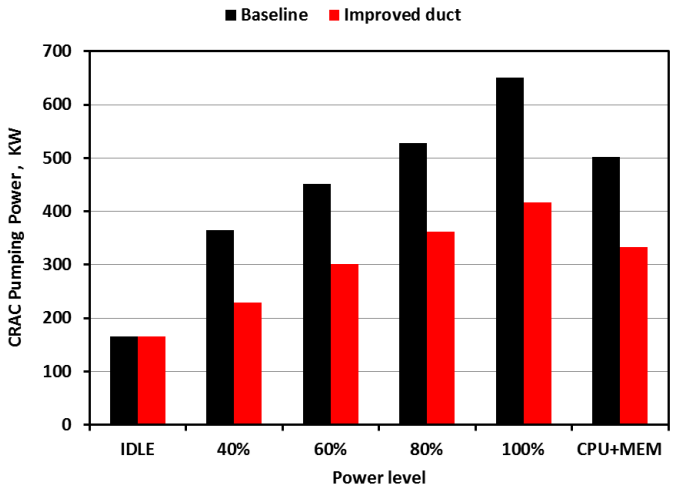

Figure 7.4. Savings achieved in CRAC Pumping power.

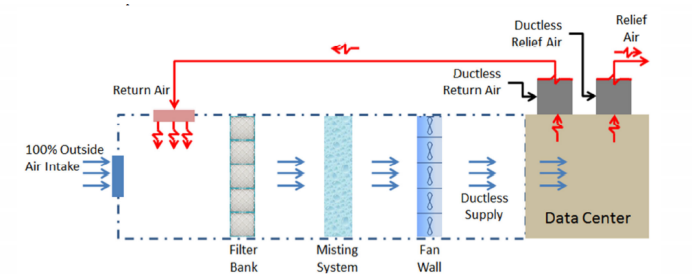

Figure 7.5. Facebook Prineville datacenter layout.

peratures during cold climates. The air after getting filtered is sent to evaporation cooling/Humidification room having misting system. The air is then passed through

the fan wall and is sent to cold aisle of the datacenter room. The air collects heat from the IT equipment and is sent to hot aisles. The exhaust is then returned to the atmosphere or to the intake corridor. The datacenter consists of 14 arrays of direct drive plenum fans employed with VFDs (Variable Frequency Drives to minimize operating costs [16]. In order to extrapolate the savings in fan power consumption and flow rates at server level to highly efficient datacenter, fan laws are used. The savings in flow rate achieved is co-related to savings in fan wall power consumption with the aid of fan laws. It is known that 20% savings in flow rate leads to 50% savings in fan power consumption. 31-37% savings in flow rate by improving the duct design leads to 68-75% savings in fan wall power consumption in highly efficient datacenter. Table 7.5 presents the savings achieved in fan wall power consumption

7.2.2 Savings in water power consumption

Enormous usage of water in datacenters is driving the datacenter operators towards the research on water management. In this paper, considerable savings in water consumed by the plant is accomplished in the improved duct case. In order to calculate the amount of water consumed by the direct evaporation units in a datacenter working on air side economization , cellulose wet cooling pads studied by Antonio Franco and team [17] to evaluate energy efficiency in green house, is employed .They conducted a study on corrugated cellulose pads with angle of incidence 450-450 and with a cross sectional area of 0.01m as shown in Figure 7.6 and reported that the saturation efficiency increases with reduction in velocity and water consumption decreases with the decrease in velocity of air. Therefore it results in higher saturation efficiency and reduced water consumption in improved duct case since the velocity is reduced by 37.5% when compared to baseline

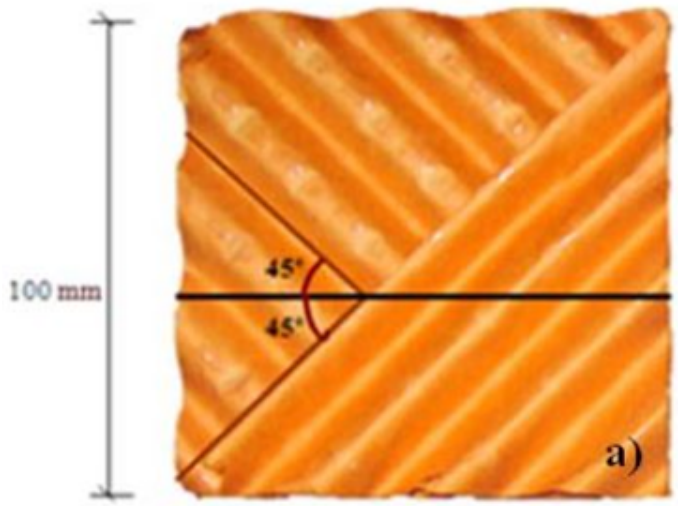

Figure 7.6. Cellulose wet cooling pad with angle of incidence 45°-45° .

Equations used to calculate Water consumption and saturation efficiency of the cellulose wet cooling pads is shown below[15],

Saturation efficiency (%): $Y = -0.2356x^2 - 2.1839x + 72.341$

Water consumption ($L\ h^{-1}\ m^{-2}\ \ ^{\circ}C^{-1}$) : Y=1.6032x+0.1805

Where m is the area of the cellulose cooling pads, °C is the temperature difference of the air entering and exciting the wet cooling pads, h is in hours. In this paper server inlet temperature (Temp of the air exiting the cooling pads) of 24.5°C is maintained throughout. Air inlet temperature is selected as per ASHRAE standards [9], however the estimation of relative savings percentage between the baseline study and improved duct study will be identical with respect to any dry bulb temperature selected. 33% of maximum savings in water consumption is achieved in the improved duct case which saves enormous capital investment used for storing and performing water treatments before supplying the water to the data centers.

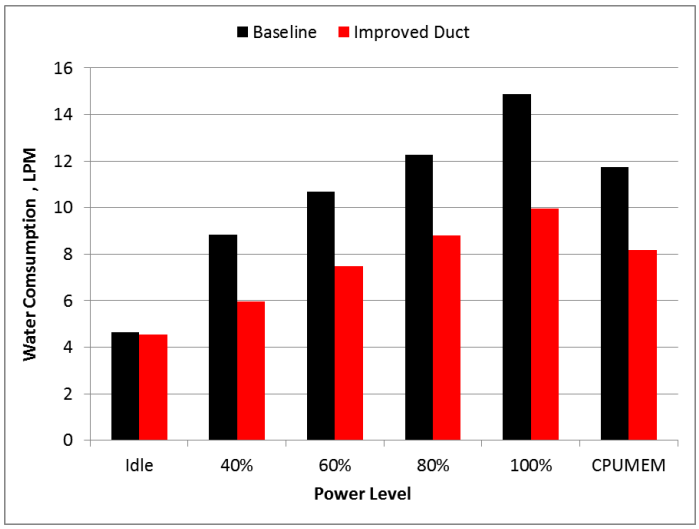

Figure 7.7. Savings achieved in water consumption of the plant by improving the duct.

CHAPTER 8

Conclusion and Future Work

8.1 Conclusion and Discussion

Flow and Thermal experimental test results obtained by testing the server is deployed to calibrate a computational fluid dynamics model using a commercially available CFD code. The resulting calibrated model is utilized to parametrically improve the ducting system to obtain efficient air distribution pattern at the same time to counteract the effects of thermal shadowing. Computationally improved duct is prototyped using acrylic sheets and experimentally tested to evaluate the savings achieved in fan power consumption, flow rates, fan speeds and acoustic noise levels. The savings achieved are listed below,

1. 23.5-40% of savings is achieved in cooling power consumption as a result of improved duct.

2. 28 - 33% savings in flow rates as a result of 22%-26% reduction in fan speeds

3. 6.5 -17% reduction in Acoustic noise levels which is of vital importance in maintaining productive work space for datacenter workers.

Further savings achieved by extrapolating the savings to facility layout of a data center are as follows,

1. 31-37.5% and 68-75% savings in total pumping power in traditional data centers and highly efficient datacenters respectively.

2. 28.5% to 33.2% savings in water flow rate is achieved. 10-19 CRAC units required to cool the datacenter can be shut off due to reduction in flow rates

8.2 Future work

Servers with baseline and improved duct can be studied at various inlet temperatures according to ASHRAE set limits, to estimate the behavior of savings at elevated temperatures.

REFERENCES

[1] J. G. Koomey, "My new study of data center electricity use in 2010," p. 1, 2011.

[2] S. Lacey, "Data Center Efficiency May Be Getting Worse," 2013. [Online]. Available: http://www.greentechmedia.com/articles/read/are-data-centers-getting-less-energy-efficient

[3] R. A. Steinbrecher, "Data Center Environments ASHRAEs Evolving Thermal Guidelines," *ASHRAE*, pp. 42–49, 2011.

[4] Energy Network Power, "Energy Logic 2.0 New Strategies for Cutting Data Center Energy Costs and Boosting Capacity," p. 2, 2007.

[5] S. Madera, "How do I cool high-density racks?" 2007. [Online]. Available: http://searchdatacenter.techtarget.com/feature/How-do-I-cool-high-density-racks

[6] T. Yuan, "Computational Modelling of Flow Bypass Effects on Straight Fin Heat Sink in Rectangular Duct," in *SEMI-THERM*, 1996, pp. 164–168.

[7] S. L. Rong, H. C. Huang, and W. Y. Chen, "A Thermal Characteristic Study of Extruded Heat Sinks," in *Sixth IEEE SEMI-THERMm Symposium*, 1990, pp. 95–102.

[8] K. S. Lau and R. L. Mahajan, "Effects of Tip Clearance and Fin Density on the," *IEEE*, vol. 12, no. 4, pp. 757–765, 1989.

[9] J. Ning, "Intel Server in Open Rack Hardware v0.3 (MB-draco-genam-0.3)," in *Intel*, 2013.

[10] P. Jay, "Data Center v1.0," 2011. [Online]. Available: http://www.opencompute.org/assets/Uploads/DataCenter-Mechanical-Specifications.pdf

[11] V. Pandian, "Development of Detailed Computational Flow Model of High End Server," University of Texas at Arlington, Tech. Rep. December, 2012.

[12] Future Facilities, "6SigmaET R8." [Online]. Available: http://www.air-think.com.tw/uploads/6/1/7/6/6176073/6sigmaet-whatsnew-r8.pdf

[13] J. L. L. Clemens, "CFD Simulations in Electronic Systems: A Lot of Pitfalls and a Few Remedies," in *IEEE*, 2002, pp. 366–382.

[14] J. Bean, "SERIES," in *White Paper*, vol. 18, no. January, 2010, pp. 1–25.

[15] M. Iyengar and R. Schmidt, "Analytical Modeling for Thermodynamic Characterization of Data Center Cooling Systems," *Journal of Electronic Packaging*, vol. 131, no. 2, p. 021009, 2009.

[16] R. Eiland, J. Fernandes, B. Gebrehiwot, M. Vallejo, D. Agonafer, and V. Mulay, "Air Filter Effects on Data Center Supply Fan Power," in *ITHERM*, 2012, pp. 377–384.

[17] A. Franco, D. Valera, and A. Peña, "Energy Efficiency in Greenhouse Evaporative Cooling Techniques: Cooling Boxes versus Cellulose Pads," *Energies*, vol. 7, no. 3, pp. 1427–1447, Mar. 2014.

BIOGRAPHICAL STATEMENT

Divya Mani received her Bachelor's Degree in Mechanical Engineering from Visvesvaraya Technological University,India in June 2012. She received her Master of science degree in Mechanical engineering from University of Texas at Arlington in December 2014.

During her masters program she conducted her research in the field of thermal management under Dr.Derege Agonafer.She has indulged herself in various industry collaborated projects and gained extensive experience working in laboratory environment. She has worked with both experimentation and computational characterization of rack mount servers.

She worked as a Graduate Teaching Assistant under Dr.Ratan Kumar for Finite Elemental Methods during her final semester in University of Texas at Arlington.